Published in final edited form as:
J Biomed Mater Res A. 2010 May ; 93(2): 673–686. doi:10.1002/jbm.a.32485.

Patterning N-type and S-type Neuroblastoma Cells with Pluronic F108 and ECM Proteins

Joseph M. Corey, **Caitlyn C. Gertz**, **Thomas J. Sutton**, **Qiaoran Chen**, **Katherine B. Mycek**, **Bor-Shuen Wang**, **Abbey A. Martin**, **Sara L. Johnson**, and **Eva L. Feldman**
Department of Neurology The University of Michigan 5013 BSRB 109 Zina Pitcher Place Ann Arbor, MI 48109-2200

Abstract

Influencing cell shape using micropatterned substrates affects cell behaviors, such as proliferation and apoptosis. Cell shape may also affect these behaviors in human neuroblastoma (NBL) cancer, but to date, no substrate design has effectively patterned multiple clinically important human NBL lines. In this study, we investigated whether Pluronic F108 was an effective anti-adhesive coating for human NBL cells and whether it would localize three NBL lines to adhesive regions of tissue culture plastic or collagen I on substrate patterns. The adhesion and patterning of an S-type line, SH-EP, and two N-type lines, SH-SY5Y and IMR-32, were tested. In adhesion assays, F108 deterred NBL adhesion equally as well as two anti-adhesive organofunctional silanes and far better than bovine serum albumin. Patterned stripes of F108 restricted all three human NBL lines to adhesive stripes of tissue culture plastic. We then investigated four schemes of applying collagen and F108 to different regions of a substrate. Contact with collagen obliterates the ability of F108 to deter NBL adhesion, limiting how both materials can be applied to substrates to produce high fidelity NBL patterning. This patterned substrate design should facilitate investigations of the role of cell shape in NBL cell behavior.

Introduction

Cell shape and cytoskeletal tension exert powerful effects on cell behavior and fate [1–3]. Using micropatterned substrates, investigators have shown that controlling cell shape can cause a cell to switch from proliferation to apoptosis [4] or from proliferation to differentiation [2], change the speed of cell migration [5,6], and encourage differentiation of cells to form tissues [2]. The regulation of these behaviors is not only vital to tissue and organ formation during development, but is also important for the development of successful tissue-engineering applications. Moreover, abnormalities in cell adhesion, proliferation, apoptosis, differentiation, and migration are central to the pathophysiology of many diseases. All of these processes are dysfunctional in cancer [7–10], therefore studying the influence of cell shape and cytoskeletal tension in cancer cells may lead to a new understanding of cancer pathophysiology.

Neuroblastoma (NBL) cancer, a lethal disease accounting for 8% to 10% of all childhood cancers, is the most common malignant disease of infancy [11]. We have studied how the biochemical components of the tumor microenvironment affect NBL adhesion [12,13], proliferation [14,15], migration [13,16], differentiation [17], and apoptosis [18,19]. However, using micropatterned substrates to simultaneously study the influence of extracellular matrix (ECM) biochemistry and cell shape on human NBL behavior could improve our

coreyj@umich.edu .

understanding of how biochemical constituents and geometric architecture of the microenvironment combine to affect human NBL tumorigenesis and metastasis.

Human NBL cells occur in three different subtypes, S-type, N-type, and I-type, each with distinct morphologies and behaviors. S-type cells resemble glial precursor cells, are highly substrate adherent, and are non-invasive. N-type cells have a neuronal morphology, are less substrate adherent, and are highly invasive 20. I-type cells have an intermediate morphology and mixed properties of N- and S-type cells. They frequently grow as mixtures of both of these cell types in culture. Some I-type lines behave as stem cells in that they can develop into either S- or N-type cells 21. A thorough investigation into the effects of cell morphology on NBL behavior would require experiments with all three subtypes. The differences in substrate adherence and invasiveness between S- and N-type cells lead us to speculate that they would behave differently as their cell shape is controlled by substrate micropatterns. But to perform comparative experiments on cells from these types, there must be a patterned substrate design that effectively localizes all three types of human NBL cell lines.

Many patterned substrates have been developed that could serve as a basis for experiments to alter NBL cell morphology 22¯31. These various patterned substrate designs were produced using different adhesive and anti-adhesive materials. While NBL cells have been grown on these substrates, inferring which materials would successfully localize both N- and S-type cell lines is not straightforward for several reasons. First, none of the studies tested more than one NBL line. Among the six lines tested, only 2 human cell lines were used, the I-type line SK-N-SH (3 studies) and N-type line SH-SY5Y (2 studies). None of these studies were tested with S-type cells, the most adhesive of all the types. Second, because of the wide variation of adhesiveness among different human NBL cell types, there is no way to clearly discern which combinations of adhesive and anti-adhesive materials will effectively pattern all of them. For example, alkylsilane and aminosilane patterns have been shown to effectively localize I-type SK-N-SH cells 26،27،30 and primary neurons 27،32،33. However, when we applied these patterns to human NBL cells in our laboratory, the localization of both SH-SY5Y cells (N-type) and SH-EP cells (S-type) was poor. Since effective cell localization occurs only when cells migrate to the adhesive pattern from the less adhesive background areas, we concluded that we needed to create a more highly anti-adhesive background that could effectively deter all three cell types.

Among the many anti-adhesive surface coatings demonstrated to repel cells are the Pluronics. Pluronics are diblock poly(propylene oxide)-poly(ethylene oxide) (PPO-PEO) or triblock (PEO-PPO-PEO) copolymers that adsorb to hydrophobic surfaces, such as tissue culture plastic, and extend hydrophilic tails that prevent protein adsorption and therefore cell adhesion 34¯36. They are anti-adhesive to primary hepatocytes 36, endothelial cells 6،37, and sensory neurons38, as well as fibroblast (NIH-3T3)36, pre-adipocyte (3T3-L1)37, pheochromocytoma (PC-12) 35،39 and Schwann (MSC80) cell lines 35،39. However, Pluronics have never been tested with human NBL cells. In culture, Pluronics last longer than other hydrophilic anti-adhesives 37, and they can be patterned alone or in combination with proteins using microfluidic methods 6،36, photolithography 36, microcontact printing of proteins 6،40, or by competitive simultaneous adsorption with a protein on heterogenous plastic surfaces 35،39. They can also be modified with fibronectin to promote desired cell adhesion and resist adsorption of undesired serum proteins 38. Their ease of use and commercial availability makes them more attractive than coatings that require special syntheses 4،22،23،41،42 or surface modification prior to their attachment 4،41،42.

The present study examines the suitability of Pluronic F108 as an anti-adhesive coating for both S-type and N-type cells on patterns with tissue culture plastic and ECM protein-coated

adhesive regions. We found that SH-EP (S-type) and SH-SY5Y (N-type) cells adhere not only to ECM proteins and polylysine, but also to uncoated tissue culture plastic and bovine serum albumin. Using both of these cell lines along with another N-type cell line (IMR-32), we found that F108 is an effective anti-adhesive for all tested NBL cell lines on uniformly coated surfaces, and is effective in promoting NBL localization to tissue culture plastic on microfluidic-patterned substrates.

The main stromal components associated with NBL tumors and their chief site of metastasis, bone, are the extracellular matrix proteins fibronectin and collagen 43. Therefore, relevant substrate patterns to study NBL pathophysiology should include at least one of these proteins. To produce patterns of ECM proteins with a Pluronic background, we tested four alternative schemes inherent in using microfluidics to pattern two materials and we measured their differential adhesion. Patterning the adherent protein followed by flooding (completely covering) with Pluronic produces the best cellular localization. Using this scheme, all three NBL cell lines pattern well. Lastly, we show that the patterns can localize cells and restrict cell shape of most cells for over one week. This study is the first to use Pluronics for patterning NBL, as well as the first to pattern both N and S-type NBL cell lines using a single patterning technique. We show that F108 and ECM proteins can be patterned to allow the study of how ECM geometry and biochemistry affect human NBL growth and metastasis.

Materials and Methods

All chemical reagents were purchased from Sigma-Aldrich (St. Louis, MO) unless otherwise stated.

Preparation of Uniform Substrates

Protein-coated Surfaces—Uniform protein-coated surfaces were prepared on 24-well plates (Corning, Corning, NY). Proteins were prepared according to the company datasheet instructions and applied at the following concentrations: laminin from Engelbreth-Holm-Swarm sarcoma at 25 μg/mL, collagen I at approximately 100 μg/mL, BSA at 2.5 wt. %, poly-L-Lysine (mol. wt. > 300,000) at 10 μg/mL. Pluronic F108 prill was generously donated by BASF Corporation (Florham Park, NJ), diluted to 1% in distilled, deionized water, and used within 1 week.

Silane Deposition—Silanes were coated on VWR glass cover slips (22 × 22 mm, No 1½). All cover slips were cleaned in 20% methanol solution for 20 min in a bath sonicator, rinsed liberally in distilled water, immersed overnight in piranha etch [7:3 sulfuric acid (70%):hydrogen peroxide (30%)], rinsed liberally, and baked in an oven to dry. Cover slips coated with trichloro(1*H*,1*H*,2*H*,2*H*-perfluorooctyl) silane (13F) were immersed in a 0.5 % solution in anhydrous toluene (both from Sigma-Aldrich) for approximately 30 min, and rinsed in 2 changes of toluene 32. Cover slips coated with phenyltrichlorosilane (PTCS) were immersed in 5% for 15 min, and rinsed in 2 changes of toluene 33. Dimethyldichlorosilane (DCDMS) was applied in the vapor phase by placing clean cover slips together with a small drop of the silane on a separate glass slide and then applying a vacuum for 7 min. All silane reactions were completed by baking the cover slips at 130°C for 1 h.

Cell Culture

SH-EP, SH-SY5Y, and IMR-32 cells were maintained in Falcon tissue culture plates (BD Biosciences, Bedford, MD) using Dulbecco's modified Eagle's Medium (DMEM) (Invitrogen Corporation, Carlsbad, CA) supplemented with 10% calf serum (Hyclone,

Logan, UT). Cells were plated on all substrates at 50 cells/mm^2 and in this media unless otherwise stated.

Adhesion Assays

SH-EP cells were used for most adhesion assays because they are more highly adhesive and would better test the ability of anti-adhesive candidates to deter cell adhesion. Cells were plated and grown overnight, fixed in 4% paraformadehyde, and stained with Coomassie blue to allow each cell border and nucleus to be seen easily. For experiments on well plates, 3 wells with each coating were used and 3 adjacent fields in each well counted. Near the edges of the well plates, there was a margin where cells adhered in greater numbers. The first field was positioned to the right of this margin nearest the left edge of the well. For experiments using glass cover slips, 3 substrates of each coating variation were used. Ten adjacent fields were counted, with the first field selected away from the edge of the cover slip. The cells counted lay in a field delineated by a square reticle with an area of 2.25 mm^2. Data were analyzed using ANOVA and Tukey's multiple comparison tests with Prism software (www.graphpad.com).

Cell Area Measurements

SH-EP, SH-SY5Y, and IMR-32 cells were cultured at 50 cells/mm^2 on 60 mm diameter tissue culture dishes that were either uncoated or coated with collagen. The next day cells were fixed with 4% paraformaldehyde and stained with phalloidin (Invitrogen, Carlsbad, CA) (1:200) to visualize actin fibers and bisbenzamide (1 μg/mL) to visualize cell nuclei. The areas of the cell and nucleus were measured using the area tool in Metamorph software (Molecular Devices, Sunnyvale, CA). The area encompassing the phalloidin staining was defined as the cell area and the area encompassing the bisbenzamide staining defined as the nucleus area. Only cells not in contact with other cells were measured. The number of cells measured per condition was 47 ± 13 (avg ± st. dev.) Data were analyzed using ANOVA and Tukey's multiple comparison tests with Prism software.

PDMS Stamps

To create stamps, Autocad software was used to draft a pattern mask as arrays of parallel lines of varying width. CAD/Art Services, Inc. (Bandon, OR) printed the Autocad files on transparency masks. To make molds used in stamp formation, mask patterns were first transferred to silicon wafers coated with SU-8 photoresist (MicroChem Corp, Newton, MA). The resist was exposed to UV light and developed to leave a 30 to 80 μm profile of the pattern on the wafer. Dr. Nobuyuki Futai from the University of Michigan Department of Biomedical Engineering generously performed photolithography with reagents and equipment provided by Dr. Shuichi Takayama. 13F silane was reacted in the vapor phase to render molds non-adhesive to the PDMS during polymerization. Stamps were made by polymerizing Sylgard 184 (Dow Corning, Midland, MI) on the molds and soft-curing according to package directions. Stamps used in early stages of this work were made by Xiaoyue Zhu and generously donated by Dr. Shuichi Takayama.

Patterning of Pluronic F108

Rectangular holes were cut in the stamps as inlets and outlets for solutions of protein or Pluronic F108. The stamp was pressed to contact the surface of a 60 mm diameter tissue culture dish or DCDMS-coated cover slip. A small drop of solution was placed in one of the holes; the liquid proceeded down the channels through capillary action or was aided by suction with a pipette bulb. Solutions were left to dry in a tissue culture hood before the stamp was removed.

Patterning of Collagen I and F108

Collagen I and F108 were patterned according to 1 of 4 schemes (Fig 4). From these schemes, there are a total of 4 surfaces that NBL cells would encounter when plated: collagen alone, F108 alone, F108-on-collagen, or collagen-on-F108. NBL cell adhesion to these candidate surfaces was measured on unpatterned tissue culture plastic as detailed above. F108 was applied for 3 h, collagen for 1 h, and the top layer of F108 (on collagen) for 10-60 min. We then normalized the adhesion data from these 4 surfaces to that of collagen alone. These normalized data were used to calculate the reduction in adhesion provided by the candidate anti-adhesive surface for each scheme as follows:

$$\text{Percent Reduction} = \frac{\text{Adhesive Surface} - \text{Anti-adhesive Surface}}{\text{Adhesive Surface}} \times 100\%$$

To construct patterns of both materials, collagen was patterned using the PDMS stamps as described above in 60 mm tissue culture dishes or on DCDMS-coated glass cover slips. FITC-conjugated collagen was used in select experiments to allow visualization of the pattern. After drying for a minimum of 3 d, 1% F108 solution was flooded to cover the entire surface for varying durations. Alternatively, F108 was flooded, the solution aspirated from the surface, then collagen I patterned.

Cell Patterning

Cells were plated on patterned substrates at 50 cells/mm^2. To assess patterning quality, cells were grown overnight, fixed in 4% paraformaldehyde, and stained with either red or green phalloidin (1:200) to visualize actin fibers and bisbenzamide (1 μg/mL) to visualize cell nuclei. To assess duration of cell patterning, cells were plated on patterned substrates at 50 cells/mm^2 and repeatedly photographed every 3-4 d until cells died or patterning quality diminished significantly. SH-EP cells were grown in DMEM with 0.3% calf serum to reduce proliferation 44 and SH-SY5Y cells were grown in Neurobasal medium with B27 supplement (both from Invitrogen) to enhance neurite outgrowth and reduce proliferation. The experiment was terminated when the cells overgrew the pattern or died.

Results

Adhesion of Neuroblastoma Cells on Candidate Surface Coatings

Cells pattern due to an adhesive difference between the pattern and the background. We therefore surveyed adhesive and anti-adhesive candidate materials for their effects on NBL cell adhesion. In the first experiment, collagen I, laminin, poly-L-lysine, and uncoated tissue culture plastic (TCP) were adhesive candidates while bovine serum albumin (BSA) was the anti-adhesive candidate. On these substrates, SH-EP cells were plated, grown overnight, fixed, stained, and counted. Collagen and laminin produced significantly greater adhesion than polylysine, tissue culture plastic, and BSA (Fig 1A; $p < 0.01$). However, BSA did not significantly reduce cell adhesion when compared to polylysine and TCP, suggesting that it would not serve effectively as an anti-adhesive surface. SH-SY5Y cell adhesion to these substrates mirrors that of SH-EP cells (data not shown). We next tested Pluronic F108 as an anti-adhesive surface. F108 significantly reduced SH-EP cell adhesion by 95% compared to collagen I and 94% compared to tissue culture plastic (Fig 1B; $p < 0.001$).

We then compared F108 to two additional anti-adhesive coatings, PTCS and 13F. PTCS and 13F are silanes that react to form covalent bonds with glass, but do not react with plastic. Conversely, F108 adsorbs only on hydrophobic surfaces, making it ineffective when applied to unmodified glass. Therefore, a contrast in the effects of these three anti-adhesive coatings

on cell adhesion might be attributable to the substrate underlying the coating material. To make the comparison impartial, all coatings were applied to glass cover slips; glass coverslips were made hydrophobic by reaction with DCDMS to allow F108 coating. For these experiments, we measured the adhesion of two NBL lines, SH-EP (Fig 2A) and SH-SY5Y (Fig 2B). No difference in cell adhesion was observed among the anti-adhesive coatings PTCS, 13F, and F108 for either NBL line (Fig 2). Furthermore, for F108, the underlying substrate is irrelevant: F108 adsorbed to DCDMS-glass repels NBL cells equally as well as F108 adsorbed to tissue culture plastic (Fig. 2). DCDMS-glass alone does not repel NBL cells as well as F108 on DCDMS-glass (Fig 2; $p < 0.001$ for SH-EP and $p < 0.01$ for SH-SY5Y), further confirming the anti-adhesive effect of F108.

F108 Confines NBL Cells to Patterned Stripes

Given the significantly increased NBL cell adhesion to tissue culture plastic compared to F108, we hypothesized that NBL cells cultured on alternating stripes of these two materials would localize on the tissue culture plastic. Alternating stripes of F108 and tissue culture plastic were made using a microfluidic technique (Fig 3A). Three NBL cell lines with varying cell-surface adhesiveness, SH-EP (Fig 3B, C), SH-SY5Y (Fig 3D), and IMR-32 (Fig 3E) effectively pattern onto the tissue culture plastic stripes within 24 h. The quality of patterning is equal for all 3 NBL lines tested. In addition, neurites extending from serum-starved, differentiated SH-SY5Y cells are primarily confined to the adhesive stripes as seen in the live phase-contrast image (Fig 3D). N-type cells, SH-SY5Y (Fig 3D) and IMR-32 (Fig 3E), adhere to each other when localized on stripes of tissue culture plastic, but appear completely within the F108 borders. Pluronic F108 not only restricts cell location, but also cell shape. Patterned SH-EP cells are narrower on the narrower stripes of tissue culture plastic (Fig 3B).

Producing Collagen and F108 Double Patterns

In creating patterns of both extracellular matrix proteins (ECM) and F108 with a microfluidic stamp, it is necessary to pattern one of the materials and flood the other, resulting in either the pattern or background coated with both materials. Surfaces coated with both materials may produce cell adhesion different from that produced by either material alone. To evaluate the interaction between collagen I and F108, four schemes were designed for application of the two materials (Fig 4A). SH-EP cell adhesion was then measured on the 4 possible candidate surfaces resulting from the 4 schemes: collagen I alone, F108 alone, collagen-on-F108, and F108-on-collagen (Fig 4A). While F108 alone resisted cell adhesion, F108 apparently did little to resist collagen (collagen-on-F108), since the number of cells adhering to that surface is statistically equal to those adhering to collagen alone (Fig 4B). Furthermore, applying F108 after collagen actually increased SH-EP cell adhesion compared to applying F108 before collagen (collagen-on-F108) (Fig 4B; $p < 0.05$). Most published work in creating patterns of an ECM protein and Pluronic F108 has used fibronectin as the ECM protein. Therefore, we also tested these surface coating schemes with fibronectin. Compared to the analogous surfaces tested with collagen in Figure 4, each candidate surface coated with fibronectin and/or F108 produced an essentially identical adhesion of SH-EP cells (data not shown).

We sought to identify which patterning application scheme would produce the highest difference in cell adhesion between the candidate adhesive and anti-adhesive regions. To do this, we calculated the net reduction in SH-EP adhesion (Fig 4C) produced by the candidate anti-adhesive surface compared to the candidate adhesive surface for the four schemes illustrated in Fig 4A. We found that the application schemes producing a substantial difference in cell adhesion between the two candidate surfaces must contain F108 alone, requiring that collagen is patterned and F108 is flooded, in either order (schemes 1 and 2;

Fig 4C). Note that in both of these schemes F108 is not contacted by collagen either before or after its application step.

We then asked if it were possible to limit the pro-adhesive effect of collagen I (Fig 4B) by shortening the time that collagen I was applied. In schemes 2 and 3, collagen is applied to regions already coated by F108. We asked whether F108 would resist collagen deposition even for short periods of collagen application. SH-EP adhesion results indicate that even at 5 min of application time, collagen substantially increases adhesiveness compared to F108 alone (Fig 5A; $p < 0.001$). F108 is unable to resist collagen I application even after 5 minutes of collagen exposure. This situation favors a high adhesive difference between the pattern and background, important in making scheme 2 successful, but limiting the chances of success for scheme 3.

For steps where F108 is flooded to cover the background areas either before (scheme 2) or after (scheme 1) patterning collagen I, the ability of F108 to reduce cell adhesion was tested as a function of its application time (Fig 5B). At only 1 min of application time, F108 decreases the adhesion of SH-EP cells compared to unmodified tissue culture plastic by 80%, increasing to 85% at 6 min, 89% at 10 min, and 96% at 60 and 180 min (Fig 5B; $p < 0.001$). These results suggest the effectiveness of cell patterning by scheme 1 or 2.

NBL Cells on Double Patterns Adhere to Collagen and Avoid F108

Using scheme 1, patterning FITC-labeled collagen and then flooding F108, the ability of collagen I/F108 double patterns to control NBL cell adhesiveness was tested. All three cell types localized to collagen stripes and avoided F108 stripes, although S-type SH-EP cells appear to localize more poorly to the patterned collagen (Fig 6B) when compared to N-type SH-SY5Y and IMR-32 cells (Fig 6C, D respectively). However, on collagen patterns without F108 (Fig 6A) many more SH-EP cells localized on the background regions of TCP compared to when F108 was applied (Fig 6B). This demonstrates the necessity of using an anti-adhesive material to localize cells to the collagen stripes. On patterns produced using schemes 3 and 4, SH-EP cells comply to both adhesive and background regions (data not shown).

Cell Size Differs among NBL Lines and Is Affected by Surface Composition

On both patterned and uniform surfaces, we noticed a variation in size among the three NBL lines, therefore we measured the size of each cell line on both uniform TCP and collagen I (Table I). We found that each cell line exhibited significantly greater cell spreading on collagen than on TCP (SH-EP $p<0.001$, SH-SY5Y and IMR-32 $p<0.05$). Similarly, the area of the nucleus was significantly greater on collagen than TCP for both SH-EP ($p<0.001$) and IMR-32 cells ($p<0.05$) but not SH-SY5Y cells. The N-type cells, SH-SY5Y and IMR-32, had equal cell and nuclear size on both surfaces while SH-EP cell area was almost twice as large as the area of the other two lines, whether on collagen ($p<0.001$) or TCP ($p<0.001$). The average area of the SH-EP nucleus was also significantly greater than the N-type cell lines on both collagen ($p<0.001$) and TCP (SH-SY5Y $p<0.05$, IMR-32 $p<0.001$).

F108 Pattern Duration

A robust patterning system should work for long-term culture applications. SH-EP cells were cultured on stripes of F108 on tissue culture plastic in 0.3% serum to reduce their growth rate. SH-EP cells remain well-patterned on the stripes of tissue culture plastic for up to approximately 1 week, with initial pattern breakdown occurring at 9-10 d and becoming more pronounced at 12 d (Fig 7A-C). SH-EP cells start to die by 14 d in most cases, but some remain alive and pattern past 21 d (data not shown). SH-SY5Y cells, grown in Neurobasal with B27 supplement, are reliably confined by F108 for much shorter periods of

time (Fig 7D-F). By day 4, some of the cells have encroached on the F108 stripes (Fig 7D). This becomes more pronounced by day 7 (Fig 7E), although the majority of cells remained on the stripes of tissue culture plastic. By 12 d many of the cells had died, leaving an appearance of high patterning fidelity (Fig 7F).

Discussion

The content and architecture of the tumor microenvironment play prominent roles in tumor cell behavior, affecting cell migration, invasion, and survival 45-47. However, mimicking this microenvironment *in vitro* for detailed cellular analyses has been difficult 48. The objective of this study was to develop a micropatterning technology that effectively localizes both N- and S-type NBL cells to allow a subsequent investigation of the effects of ECM geometry and biochemistry on tumor cell behavior. The question of whether restricted cell shape affects NBL behavior and how it may differ among various human NBL cell types cannot be answered without a reliable technique for effectively patterning multiple NBL cell lines. In this study, we found that Pluronic F108 confines NBL cells to more adhesive regions on substrate patterns. NBL cell patterning by F108 works for three human NBL cell lines that vary in cell-to-substrate adhesiveness. Also, by assessing NBL cell adhesion on candidate surfaces, we used Pluronic F108 along with patterned collagen to confine NBL cells to collagen-coated regions. While several studies demonstrate the ability of patterns to localize NBL cells and their neurites 22-26,28,29,31, ours is the first technique demonstrated to pattern different NBL lines of varying adhesiveness.

The adhesion of human NBL cells is easily deterred by F108, but not by BSA. In our experiments, F108 reduced adhesion of SH-EP cells, the most adhesive NBL line tested, by 94% compared to tissue culture plastic and 95% compared to collagen I (Fig 1). Similar results were seen with SH-SY5Y cells (data not shown). Not only do these results corroborate those of others who have shown that F108 deters adhesion of several primary cell types and cell lines 6,35-39, but it also shows that the adhesion of multiple lines of one tumor type are modulated by F108.

In contrast, BSA does not reduce NBL cell adhesion. BSA is frequently used as a non-adhesive control surface when measuring cell-substratum adhesion and is anti-adhesive for primary neurons 49. When used on substrate patterns, BSA deters cell adhesion enough to produce cell patterning in serum free media 50. However, the ability of BSA to deter cells from adhering is limited. Endothelial cells and 3T3-L1 pre-adipocytes grown on patterns with BSA backgrounds are effectively confined to adhesive fibronectin islands for only 2 d in serum-free media and for only 18 h in media with serum 37. We did not measure the adhesion of NBL cells on BSA in serum-free media because most NBL lines, including SH-EP cells, need at least a small amount of serum to survive. Regardless, the high adhesiveness of NBL cells to BSA precludes it as an anti-adhesive coating for NBL cells.

We compared NBL cell adhesion to Pluronic F108 with cell adhesion to phenyl- and fluoroalkyl-silanes, compounds that covalently bind to glass and render surfaces hydrophobic 51. We found that Pluronic F108 is as equally anti-adhesive as PTCS and 13F for SH-EP and SH-SY5Y cells after 1 d in culture (Fig 2). Silanes are effective anti-adhesive coatings that pattern many cell types, including primary hippocampal neurons27,32,33,52 and the SN-K-SH human NBL I-type cell line 26,27,30, the parent line of SH-EP and SH-SY5Y. These results contrasted with our early attempts to pattern NBL cells with silanes: whereas diethylenetriamine silane (DETA) grids on a PTCS background localize primary neurons 33, SH-EP cells do not comply to these patterns and SH-SY5Y cells do so inconsistently and only when differentiated in serum-free media (data not shown). This could be explained by the hydrophobicity of the PTCS background which may increase the

adsorption of serum proteins including BSA that these NBL lines find adhesive (Fig 1). The strong anti-adhesive effect of PTCS observed with primary neurons may be facilitated by the lack of serum proteins in serum-free media 27,32,33,51, though others have successfully localized primary neurons on silane patterns in serum-containing media 52. Another potential explanation for the poor compliance of SH-EP and SH-SY5Y cells to DETA/PTCS patterns may be an insufficient adhesiveness of DETA for these cells. It is possible that the adhesive or anti-adhesive silane monolayers on these patterns may have been contaminated by polymerization of the silane caused by minute amounts of water in their solvents or in the atmosphere. Silanes react so readily with water that organic solvents for silane reactions may need to be distilled in the laboratory 53 before use, and the reactions run in chambers with controlled atmosphere 32. These requirements make silanes much less robust for cell patterning compared to Pluronics, which have a long shelf life and which are typically used in aqueous solution.

Patterned Pluronic F108 effectively confines both N- and S-type NBL cells to stripes of tissue culture plastic. F108 produced better patterning of these NBL lines than did PTCS against a DETA pattern, despite their equal strength at deterring cell adhesion. Neurites of differentiating SH-SY5Y cells are mostly confined to adhesive stripes of tissue culture plastic (Fig 3D). F108 not only restricts cell location, but also cell shape. Patterned SH-EP cells assume a width consistent with the width of the stripe of tissue culture plastic (Fig 3B, C). This geometric influence on the shape of individual SH-EP cells was also observed on the N-type cells cultured in our study, SH-SY5Y and IMR-32. On uniform substrates, it is well-known that N-type cells adhere more weakly to the substrate and more strongly to each other compared to SH-EP cells. This was also observed on line patterns, on which cells of both N-type lines clustered together in groups when confined to narrow lines (Fig 3D).

We examined the four possible schemes for the microfluidic patterning of F108 and ECM proteins on the same substrate (Fig 4). Of these 4 schemes used to combine collagen and F108, schemes 1 and 2 yielded greater differences in adhesion between the candidate pattern and background surfaces than did schemes 3 and 4. This is because candidate surfaces occupied by both collagen and F108 did not deter NBL cell adhesion. Collagen overpowered the ability of F108 to deter cell adhesion. The order of collagen application appears to matter, since SH-EP adhesion to F108-on-collagen was increased compared to adhesion to collagen-on-F108 (Fig 4B). However, neither surface was more adhesive compared to collagen alone.

The higher cell adhesion seen on F108-on-collagen surfaces may result from collagen changing the orientation of F108 such that its hydrophilic tails are not oriented to deter protein, and therefore cell adhesion. Even if collagen does not occupy the entire available surface, it may prevent F108 from adsorbing to the substrate, thereby preventing its deterrence of cell adhesion. Since cell adhesion to collagen is mediated by integrins, the presence of even a minimal amount of collagen could be enough to allow focal contact formation and cell adhesion. Future studies will look to see if this observation is the result of an integrin-mediated, biochemical event or if it is simply an artifact of the technique. The high cell adhesion seen on collagen-on-F108 surfaces is consistent with the previous finding that hepatocytes adhere to surfaces where collagen is applied after F108 36. Even when applied for only 5 min (Fig 5A), collagen negates the anti-adhesive effects of F108. This finding renders scheme 3 unusable. However, had F108 impaired the ability of collagen to promote NBL cell adhesion, the differences between adhesive and anti-adhesive candidate surfaces in schemes 1 and 2 would not have been as favorable.

The interference of F108-mediated cell deterrence by collagen when the two materials are exposed to the same substrate regions is similar to that observed with adhesive amino silanes

and anti-adhesive alkyl- and phenylsilanes. In a study comparing methods of silane patterning, DETA negated the anti-adhesive effects of PTCS applied previously to the same regions of the substrate 33. Our finding of a similar relationship between collagen and F108 emphasizes the importance of precisely defining the surfaces of patterned substrates to provide cells with clear adhesive and anti-adhesive signals.

The three NBL cell lines adhered preferentially to patterned collagen surrounded by F108 (Fig 6). While these patterns are the same as those used by Li and colleagues to control the shape of vascular endothelial cells 6, this is the first demonstration of successful use of these patterns to localize cancer cells. The effective patterning of highly adhesive SH-EP cells and the less adhesive SH-SY5Y and IMR-32 cells is contingent upon producing patterns where the anti-adhesive effects of F108 are not contaminated by the presence of collagen. This technique provides a reliable method for patterning NBL cells.

We found that all three cell lines were greater in size when cultured on collagen compared to TCP. This is probably due to increased integrin binding on the collagen-coated surfaces, resulting in increased cell spreading. The cell and nuclear areas of the two N-type NBL lines, SH-SY5Y and IMR-32, were equal to each other on each surface, while S-type SH-EP cells had significantly larger areas than the N-type cells on both surfaces (Table I). These size differences likely do not affect compliance of cells to the pattern, but the extensive spreading by SH-EP cells on collagen patterns may cause them to extend on to the F108 background stripe (Fig 6B). These differences in cell size also have implications for future work which includes examining proliferation, migration, and apoptosis of different NBL lines as a function of cell shape. Our data suggest that on TCP/F108 patterns, the smaller N-type cells would need narrower TCP stripes to produce a proportional change in shape compared to SH-EP cells. Additionally, the larger cell areas on collagen suggest that adhesive stripes on collagen/F108 patterns would need to be larger than TCP/F108 patterns to produce an equivalent restriction in cell shape.

Maintenance of patterns for several days to weeks may facilitate investigations of the effects of cell-shape on cancer cell invasion and metastasis. Our results show that S-type SH-EP cells remain patterned for 9-10 days before growing on to the F108 stripes, while the N-type SH-SY5Y cells invade F108 stripes at about 4 days (Fig 7). Consistent with results from our SH-EP experiments, patterns made with Pluronic F108 break down after 1 week in a cell-independent process 37, and F108 pattern breakdown by fibroblasts occurs initially at 6 days, peaking at 14 days 36. One potential cause of F108 pattern breakdown is desorption of F108 by serum proteins 37. However, the breakdown of our patterns by SH-EP cells is roughly the same as that seen with fibroblasts, despite a significantly lower serum concentration (0.3% compared to 5%) 36,37. Furthermore, pattern breakdown by SH-SY5Y cells appears faster than SH-EP cells, despite the absence of serum. The more rapid invasion of F108 stripes by SH-SY5Y cells may be a cell-dependent process related to their inherently greater invasive capacity compared to SH-EP cells 13,20.

The ability to pattern multiple NBL cell lines using a single technique should help elucidate the role of cell shape in cancer cell behavior *in vitro*54 and *in vivo*55. In conjunction with other technologies, such as controlling co-culture of two cell types to evaluate how cell-cell contact affects cell behavior 56,57, presenting cells with ECM proteins in three-dimensional matrices 58,59, and culturing cells on surfaces with mechanical properties of the ECM 60, this patterning technique should allow better prediction of cell behavior *in situ*. Additionally, the effects of cell shape on signaling are emerging as an increasingly important area of study 61-63. The application of this Pluronic/ECM patterning method may be used to further the understanding of NBL cell behavior and pathophysiology, leading to the development of new and better therapeutics.

Acknowledgments

The authors wish to thank Professor Shuichi Takayama of the Department of Biomedical Engineering at the University of Michigan for helpful conversations and for assistance in supplying PDMS stamps with Dr. Xiaoyue Zhu, as well as for photolithography work with Dr. Nobiyuki Futai. The authors also wish to thank Dr. Kelli Sullivan and John Hayes of The Juvenile Diabetes Research Foundation (JDRF) Center for the Study of Complications in Diabetes, Morphology Image Analysis Core. This work utilized the Morphology and Image Analysis Core of the Michigan Diabetes Research and Training Center funded by NIH5P60 DK20572 from the National Institute of Diabetes and Digestive and Kidney Diseases. This work was supported by NIH T32 NSO7222 and K08EB03996 (JMC), the JDRF Center for the Study of Complications in Diabetes, and the Program for Understanding Neurological Diseases (TJS, ELF).

References

1. Huang S, Ingber DE. Shape-dependent control of cell growth, differentiation, and apoptosis: Switching between attractors in cell regulatory networks. Experimental Cell Research. 2000; 261(1):91–103. [PubMed: 11082279]
2. Dike LE, Chen CS, Mrksich M, Tien J, Whitesides GM, Ingber DE. Geometric control of switching between growth, apoptosis, and differentiation during angiogenesis using micropatterned substrates. In Vitro Cell Dev Biol Anim. 1999; 35(8):441–8. [PubMed: 10501083]
3. LeDuc P, Ostuni E, Whitesides G, Ingber D. Use of micropatterned adhesive surfaces for control of cell behavior. Methods in Cell-Matrix Adhesion. 2002:385–401.
4. Chen CS, Mrksich M, Huang S, Whitesides GM, Ingber DE. Geometric control of cell life and death. Science. 1997; 276(5317):1425–8. [PubMed: 9162012]
5. Corey JM, Wheeler BC, Brewer GJ. Compliance of hippocampal neurons to patterned substrate networks. J Neurosci Res. 1991; 30(2):300–7. [PubMed: 1798054]
6. Li S, Bhatia S, Hu YL, Shiu YT, Li YS, Usami S, Chien S. Effects of morphological patterning on endothelial cell migration. Biorheology. 2001; 38(2-3):101–8. [PubMed: 11381168]
7. Schmitt CA. Senescence, apoptosis and therapy--cutting the lifelines of cancer. Nat Rev Cancer. 2003; 3(4):286–95. [PubMed: 12671667]
8. Igney FH, Krammer PH. Death and anti-death: tumour resistance to apoptosis. Nat Rev Cancer. 2002; 2(4):277–88. [PubMed: 12001989]
9. Tenen DG. Disruption of differentiation in human cancer: AML shows the way. Nat Rev Cancer. 2003; 3(2):89–101. [PubMed: 12563308]
10. Friedl P, Wolf K. Tumour-cell invasion and migration: diversity and escape mechanisms. Nat Rev Cancer. 2003; 3(5):362–74. [PubMed: 12724734]
11. Karayalcin, G.; Paley, C.; Redner, A.; Shende, A. Neuroblastoma. In: L, P., editor. Manual of Pediatric Hematology and Oncology. Churchill Livingstone; New York: 1995. p. 419-436.
12. Meyer G, Kim B, van Golen C, Feldman EL. Cofilin activity during insulin-like growth factor I-stimulated neuroblastoma cell motility. Cell Mol Life Sci. 2005; 62(4):461–70. [PubMed: 15719172]
13. Meyer A, van Golen CM, Kim B, van Golen KL, Feldman EL. Integrin expression regulates neuroblastoma attachment and migration. Neoplasia. 2004; 6(4):332–42. [PubMed: 15256055]
14. Martin DM, Singleton JR, Meghani MA, Feldman EL. IGF receptor function and regulation in autocrine human neuroblastoma cell growth. Regul Pept. 1993; 48(1-2):225–32. [PubMed: 8265811]
15. Meghani MA, Martin DM, Singleton JR, Feldman EL. Effects of serum and insulin-like growth factors on human neuroblastoma cell growth. Regul Pept. 1993; 48(1-2):217–24. [PubMed: 8265810]
16. van Golen CM, Schwab TS, Ignatoski KM, Ethier SP, Feldman EL. PTEN/MMAC1 overexpression decreases insulin-like growth factor-I-mediated protection from apoptosis in neuroblastoma cells. Cell Growth Differ. 2001; 12(7):371–8. [PubMed: 11457734]
17. Kim B, van Golen CM, Feldman EL. Insulin-like growth factor-I signaling in human neuroblastoma cells. Oncogene. 2004; 23(1):130–41. [PubMed: 14712218]

18. Meyer A, van Golen CM, Boyanapalli M, Kim B, Soules ME, Feldman EL. Integrin-linked kinase complexes with caveolin-1 in human neuroblastoma cells. Biochemistry. 2005; 44(3):932–8. [PubMed: 15654749]
19. Schwab TS, Madison BB, Grauman AR, Feldman EL. Insulin-like growth factor-I induces the phosphorylation and nuclear exclusion of forkhead transcription factors in human neuroblastoma cells. Apoptosis. 2005; 10(4):831–40. [PubMed: 16133873]
20. Ross RA, Biedler JL, Spengler BA. A role for distinct cell types in determining malignancy in human neuroblastoma cell lines and tumors. Cancer Lett. 2003; 197(1-2):35–9. [PubMed: 12880957]
21. Walton JD, Kattan DR, Thomas SK, Spengler BA, Guo HF, Biedler JL, Cheung NK, Ross RA. Characteristics of stem cells from human neuroblastoma cell lines and in tumors. Neoplasia. 2004; 6(6):838–45. [PubMed: 15720811]
22. Yang IH, Co CC, Ho CC. Spatially controlled co-culture of neurons and glial cells. J Biomed Mater Res A. 2005; 75(4):976–84. [PubMed: 16138329]
23. Yang IH, Co CC, Ho CC. Alteration of human neuroblastoma cell morphology and neurite extension with micropatterns. Biomaterials. 2005; 26(33):6599–609. [PubMed: 15936072]
24. Corey JM, Brunette AL, Chen MS, Weyhenmeyer JA, Brewer GJ, Wheeler BC. Differentiated B104 neuroblastoma cells are a high-resolution assay for micropatterned substrates. J Neurosci Methods. 1997; 75(1):91–7. [PubMed: 9262149]
25. Soekarno A, Lom B, Hockberger PE. Pathfinding by neuroblastoma cells in culture is directed by preferential adhesion to positively charged surfaces. Neuroimage. 1993; 1(2):129–44. [PubMed: 9343564]
26. Matsuzawa M, Potember RS, Stenger DA, Krauthamer V. Containment and growth of neuroblastoma cells on chemically patterned substrates. J Neurosci Methods. 1993; 50(2):253–60. [PubMed: 8107505]
27. Matsuzawa M, Krauthamer V, Potember RS. Directional guidance of neurite outgrowth using substrates patterned with biomaterials. Biosystems. 1995; 35(2-3):199–202. [PubMed: 7488716]
28. Matsuda T, Sugawara T, Inoue K. Two-dimensional cell manipulation technology. An artificial neural circuit based on surface microphotoprocessing. Asaio J. 1992; 38(3):M243–7. [PubMed: 1457857]
29. Bohanon T, Elender G, Knoll W, Koberle P, Lee JS, Offenhausser A, Ringsdorf H, Sackmann E, Simon J, Tovar G. Neural cell pattern formation on glass and oxidized silicon surfaces modified with poly(N-isopropylacrylamide). J Biomater Sci Polym Ed. 1996; 8(1):19–39. others. [PubMed: 8933288]
30. Dulcey CS, Georger JH Jr. Krauthamer V, Stenger DA, Fare TL, Calvert JM. Deep UV photochemistry of chemisorbed monolayers: patterned coplanar molecular assemblies. Science. 1991; 252(5005):551–4. [PubMed: 2020853]
31. Ranieri JP, Bellamkonda R, Jacob J, Vargo TG, Gardella JA, Aebischer P. Selective neuronal cell attachment to a covalently patterned monoamine on fluorinated ethylene propylene films. J Biomed Mater Res. 1993; 27(7):917–25. [PubMed: 8360219]
32. Ma W, Liu QY, Jung D, Manos P, Pancrazio JJ, Schaffner AE, Barker JL, Stenger DA. Central neuronal synapse formation on micropatterned surfaces. Brain Res Dev Brain Res. 1998; 111(2): 231–43.
33. Corey JM, Wheeler BC, Brewer GJ. Micrometer resolution silane-based patterning of hippocampal neurons: critical variables in photoresist and laser ablation processes for substrate fabrication. IEEE Trans Biomed Eng. 1996; 43(9):944–55. [PubMed: 9214810]
34. Li J, Caldwell K. Plasma protein interactions with Pluronic(TM)-treated colloids Colloids and Surfaces B-Biointerfaces. 1996; 7(1-2):9–22.
35. Detrait E, Lhoest JB, Bertrand P, van den Bosch de Aguilar P. Fibronectin-pluronic coadsorption on a polystyrene surface with increasing hydrophobicity: relationship to cell adhesion. J Biomed Mater Res. 1999; 45(4):404–13. [PubMed: 10321714]
36. Liu VA, Jastromb WE, Bhatia SN. Engineering protein and cell adhesivity using PEO-terminated triblock polymers. J Biomed Mater Res. 2002; 60(1):126–34. [PubMed: 11835168]

37. Nelson CM, Raghavan S, Tan J, Chen CS. Degradation of micropatterned surfaces by cell-dependent and -independent processes. Langmuir. 2003; 19(5):1493–1499.
38. Biran R, Webb K, Noble MD, Tresco PA. Surfactant-immobilized fibronectin enhances bioactivity and regulates sensory neurite outgrowth. J Biomed Mater Res. 2001; 55(1):1–12. [PubMed: 11426386]
39. Detrait E, Lhoest JB, Knoops B, Bertrand P, van den Bosch de Aguilar P. Orientation of cell adhesion and growth on patterned heterogeneous polystyrene surface. J Neurosci Methods. 1998; 84(1-2):193–204. [PubMed: 9821651]
40. Tan JL, Liu W, Nelson CM, Raghavan S, Chen CS. Simple approach to micropattern cells on common culture substrates by tuning substrate wettability. Tissue Eng. 2004; 10(5-6):865–72. [PubMed: 15265304]
41. Prime KL, Whitesides GM. Self-assembled organic monolayers: model systems for studying adsorption of proteins at surfaces. Science. 1991; 252(5010):1164–7.
42. Singhvi R, Kumar A, Lopez GP, Stephanopoulos GN, Wang DI, Whitesides GM, Ingber DE. Engineering cell shape and function. Science. 1994; 264(5159):696–8. [PubMed: 8171320]
43. Ara T, DeClerck YA. Mechanisms of invasion and metastasis in human neuroblastoma. Cancer Metastasis Rev. 2006; 25(4):645–57. [PubMed: 17160711]
44. Singleton JR, Randolph AE, Feldman EL. Insulin-like growth factor I receptor prevents apoptosis and enhances neuroblastoma tumorigenesis. Cancer Res. 1996; 56(19):4522–9. [PubMed: 8813151]
45. Yamaguchi H, Wyckoff J, Condeelis J. Cell migration in tumors. Curr Opin Cell Biol. 2005; 17(5): 559–64. [PubMed: 16098726]
46. Raeber GP, Lutolf MP, Hubbell JA. Molecularly engineered PEG hydrogels: a novel model system for proteolytically mediated cell migration. Biophys J. 2005; 89(2):1374–88. [PubMed: 15923238]
47. Zahir N, Weaver VM. Death in the third dimension: apoptosis regulation and tissue architecture. Curr Opin Genet Dev. 2004; 14(1):71–80. [PubMed: 15108808]
48. Kim JB, Stein R, O'Hare MJ. Three-dimensional in vitro tissue culture models of breast cancer-- a review. Breast Cancer Res Treat. 2004; 85(3):281–91. [PubMed: 15111767]
49. Lochter A, Taylor J, Braunewell KH, Holm J, Schachner M. Control of neuronal morphology in vitro: interplay between adhesive substrate forces and molecular instruction. J Neurosci Res. 1995; 42(2):145–58. [PubMed: 8568915]
50. Ostuni E, Kane R, Chen CS, Ingber DE, Whitesides GM. Patterning Mamammalian Cells Using Elastomeric Membranes. Langmuir. 2000; 16(21):7811–7819.
51. Stenger DA, Pike CJ, Hickman JJ, Cotman CW. Surface determinants of neuronal survival and growth on self-assembled monolayers in culture. Brain Res. 1993; 630(1-2):136–47. [PubMed: 8118680]
52. Kleinfeld D, Kahler KH, Hockberger PE. Controlled outgrowth of dissociated neurons on patterned substrates. J Neurosci. 1988; 8(11):4098–120. [PubMed: 3054009]
53. Chang JC, Brewer GJ, Wheeler BC. A modified microstamping technique enhances polylysine transfer and neuronal cell patterning. Biomaterials. 2003; 24(17):2863–70. [PubMed: 12742724]
54. Wolf K, Wu YI, Liu Y, Geiger J, Tam E, Overall C, Stack MS, Friedl P. Multi-step pericellular proteolysis controls the transition from individual to collective cancer cell invasion. Nat Cell Biol. 2007; 9(8):893–904. [PubMed: 17618273]
55. Goth L, Rass P, Pay A. Catalase enzyme mutations and their association with diseases. Mol Diagn. 2004; 8(3):141–9. [PubMed: 15771551]
56. Bhatia SN, Yarmush ML, Toner M. Controlling cell interactions by micropatterning in co-cultures: hepatocytes and 3T3 fibroblasts. J Biomed Mater Res. 1997; 34(2):189–99. [PubMed: 9029299]
57. Nelson CM, Chen CS. Cell-cell signaling by direct contact increases cell proliferation via a PI3K-dependent signal. FEBS Lett. 2002; 514(2-3):238–42. [PubMed: 11943158]
58. Mitsiades C, Sourla A, Doillon C, Lembessis P, Koutsilieris M. Three-dimensional type I collagen co-culture systems for the study of cell-cell interactions and treatment response in bone metastases. J Musculoskelet Neuronal Interact. 2000; 1(2):153–5. [PubMed: 15758511]

59. O'Connor SM, Stenger DA, Shaffer KM, Ma W. Survival and neurite outgrowth of rat cortical neurons in three-dimensional agarose and collagen gel matrices. Neurosci Lett. 2001; 304(3):189–93. [PubMed: 11343834]

60. Aggeler J, Ward J, Blackie LM, Barcellos-Hoff MH, Streuli CH, Bissell MJ. Cytodifferentiation of mouse mammary epithelial cells cultured on a reconstituted basement membrane reveals striking similarities to development in vivo. J Cell Sci. 1991; 99(Pt 2):407–17. [PubMed: 1885677]

61. Fujita Y, Braga V. Epithelial cell shape and Rho small GTPases. Novartis Found Symp. 2005; 269:144–55. discussion 155-8, 223-30. [PubMed: 16355539]

62. Milsom C, Rak J. Regulation of tissue factor and angiogenesis-related genes by changes in cell shape. Biochem Biophys Res Commun. 2005; 337(4):1267–75. [PubMed: 16236262]

63. McBeath R, Pirone DM, Nelson CM, Bhadriraju K, Chen CS. Cell shape, cytoskeletal tension, and RhoA regulate stem cell lineage commitment. Dev Cell. 2004; 6(4):483–95. [PubMed: 15068789]

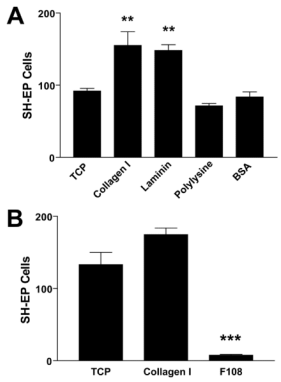

Figure 1. Adhesion of SH-EP cells to adhesive and anti-adhesive surface coatings

Cells were plated on surface coatings applied to 24-well plates for 24 h, cultured overnight, fixed, stained with Coomassie blue, and counted in a 2.25 mm^2 area. Data were analyzed using ANOVA and Tukey's multiple comparison tests. A. Collagen I and laminin promoted greater adhesion compared to tissue culture plastic, while adhesion to polylysine and bovine serum albumin was equal to that on tissue culture plastic. B. Pluronic F108 decreased SH-EP cell adhesion compared to both tissue culture plastic and collagen I. $^{**}p < 0.01$, $^{***}p < 0.001$.

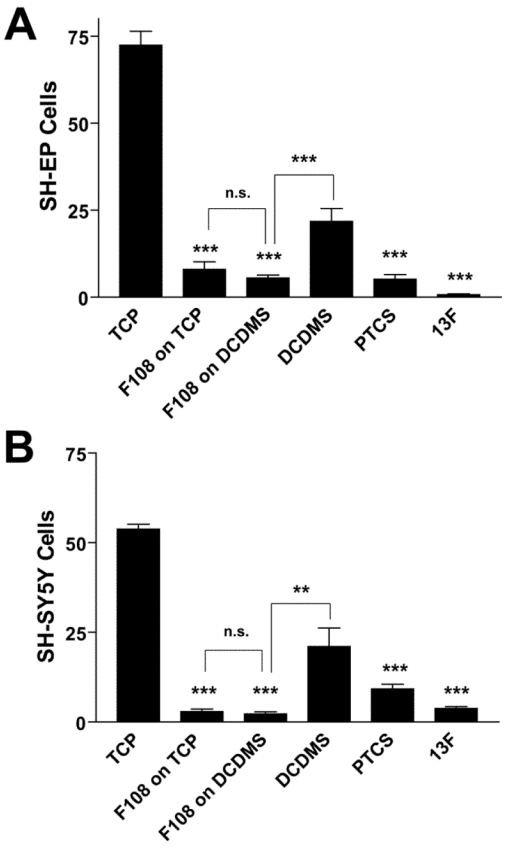

Figure 2. F108 is as anti-adhesive for NBL cells as PTCS and 13F

A. SH-EP cells. B. SH-SY5Y cells. Cells were cultured overnight on PTCS- or 13F-coated glass cover slips or on F108 adsorbed for 1 h on well plates or DCDMS-coated glass. DCDMS-coated glass without F108 was used as a control for the F108-coated glass substrate. Cells were then fixed, stained with Coomassie blue, and counted in a 2.25 mm^2 area. Data were analyzed using ANOVA and Tukey's multiple comparison tests. F108 absorbed on to tissue culture plastic and DCDMS-coated glass was as anti-adhesive as 13F and PTCS. The adhesion produced by F108 adsorbed to DCDMS-coated glass was significantly less than that on DCDMS-coated glass alone. **$p < 0.01$, ***$p < 0.001$.

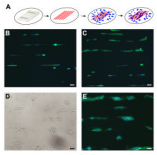

Figure 3. Patterning NBL cells with F108

A. PDMS stamp is placed in contact with a 60 mm tissue culture dish and F108 (red) is flowed through the channels. Cells (blue) land at random, detect F108 stripes and migrate to stripes of more adhesive tissue culture plastic. SH-EP cells complied to narrow (B) and wide (C) stripes of tissue culture plastic separated by stripes of F108. Both N-type cell lines, SH-SY5Y (D) and IMR-32 (E), are also patterned effectively by F108. Cells were stained with phalloidin (green) and bisbenzimide (blue). Scale bar = 50μm.

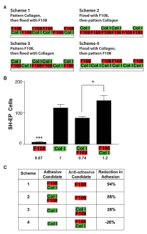

Figure 4. Schemes for making F108-collagen I double patterns

A. There are 4 possible schemes of application, each involving a patterning step of one material and a flooding step of the other. Each application scheme produces a region coated with a single material (either collagen or F108) and another region coated with both materials (collagen on F108 or F108 on collagen). These four candidate surfaces represent potential adhesive and anti-adhesive regions to cause cell patterning. B. The adhesion of SH-EP cells was evaluated on the four unpatterned candidate surfaces produced from the application schemes. Any candidate surface coated with collagen was highly adhesive; only F108 alone reduced cell adhesion. C. The adhesion produced by each candidate surface was calculated as a fraction of the cell adhesion on collagen, and then percent reduction in adhesion between the surfaces in each scheme was calculated. Schemes 1 and 2, in which collagen does not contact F108 in the application process, produced significant reductions in adhesion between the more and less adhesive candidate surfaces. *p<0.05, ***p < 0.001.

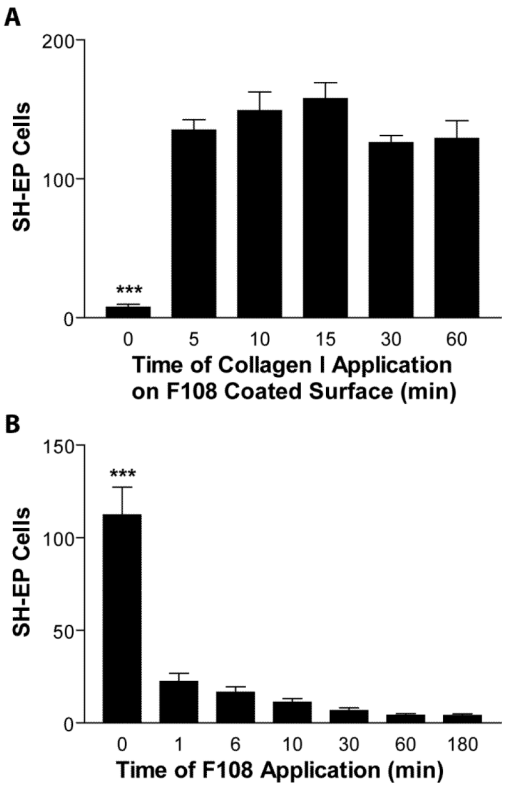

Figure 5. Collagen I applied to F108-coated surfaces negates the anti-adhesive effects of F108 on NBL cells

A. F108 was applied to tissue culture wells for 3 h, then collagen I was applied to the same wells for 5-60 min. SH-EP cells were cultured on these surfaces, fixed, stained, and counted in a 2.25 mm^2 area. SH-EP cells adhered well to all surfaces exposed to collagen, even for as little as 5 min. B. F108 was applied to tissue culture wells from 1 – 180 min. SH-EP cells were cultured on these surfaces, fixed, stained, and counted in a 2.25 mm^2 area. F108 significantly reduced cell adhesion even after being applied for only 1 min. ***$p < 0.001$.

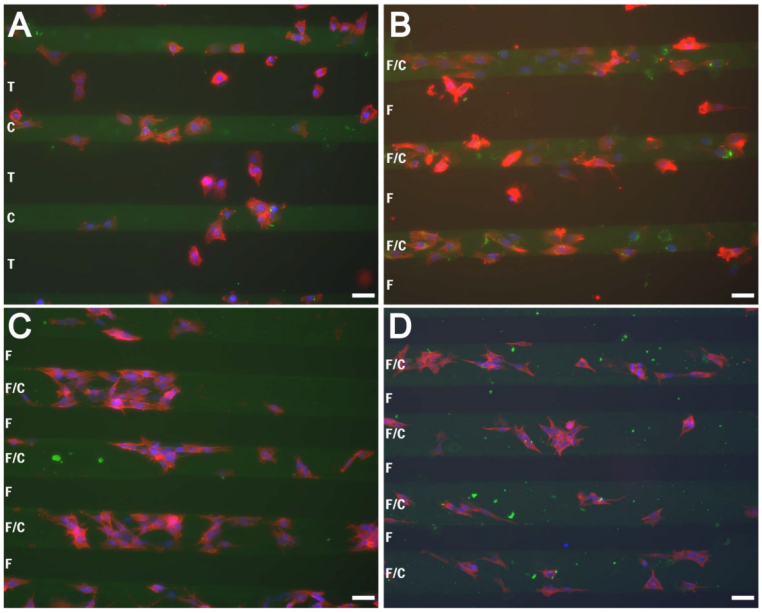

Figure 6. NBL cells comply to collagen stripes and avoid stripes of F108

Substrates were constructed by patterning FITC-labeled collagen (green stripes) in 60 mm tissue culture plates, followed by flooding with F108 (B-D). SH-EP cells fail to pattern, adhering to both collagen and tissue culture plastic when no F108 was applied (A), but localized on the patterned collagen when F108 was flooded (B). SH-SY5Y (C) and IMR-32 (D) cells also localized on the collagen/F108 stripes and avoided F108 regions. Cells were stained with phalloidin (red) and bisbenzimide (blue). T = tissue culture plastic, C = Collagen I, F = F108. Scale bar = 50μm.

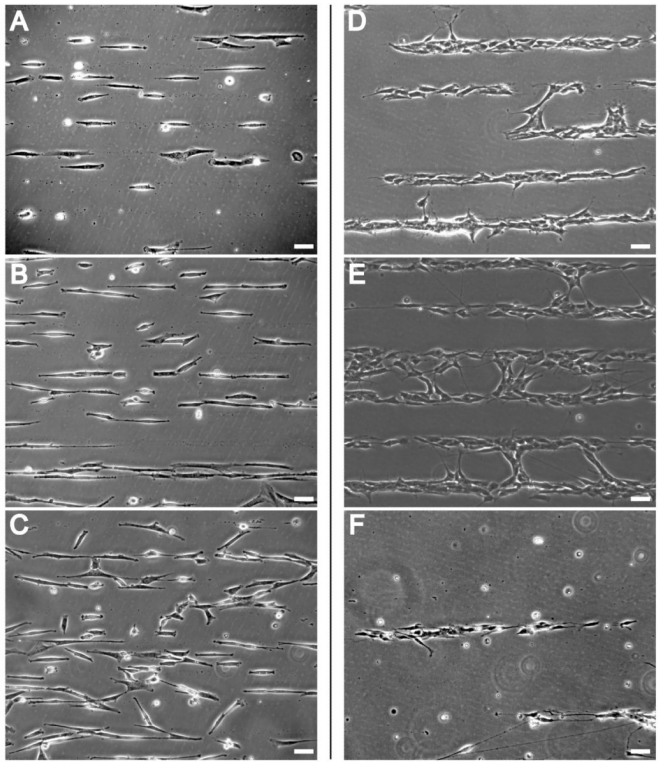

Figure 7. Long-term confinement of cells by Pluronic F108

F108 stripes were patterned in 60 mm tissue culture plates. SH-EP cells were grown in DMEM with 0.3% calf serum (A, B, C) and SH-SY5Y cells were grown in Neurobasal with B27 supplement (D, E, F). Both cell lines were plated at 50 cells/mm^2 and images were taken every 3-4 d. Images were taken from representative but not identical regions of cell patterns on the same substrates. SH-EP cells patterned well initially and remained well patterned at 3 d (A). Patterns began to break down after 10 d (B) becoming much worse by day 12 (C). SH-SY5Y cells patterned well at the onset, with some of the neurites spanning the F108 stripes. By day 4 (D), some of the cells have encroached on the F108 stripe. This becomes more pronounced by day 7 (E), although the majority of the cells remain on the stripe of tissue culture plastic. By day 12 (F), many of the cells on this substrate had died. Scale bar = 50μm.

Table I

Difference in cell size between S-type and N-type NBL. The area of phalloidin staining (cell area) and bismenzaimde staining (nucleus area) were measured for SH-EP, SH-SY5Y, and IMR-32 cells cultured on both uncoated and collagen-coated (Col I) tissue culture plastic (TCP). All cell types cultured on Col I have larger cell and nuclear areas compared to when cultured on uncoated TCP. SH-EP cells have significantly larger areas compared to the N-type cell lines on both surfaces. Statistics depicted are for comparisons among cell types cultured on the same surface. Data are presented as mean ± standard deviation.

		Cell Area (μm^2)	Nucleus Area (μm^2)
SH-EP	TCP	983.7 ± 360.4***	194.3 ± 59.6*
	Coll	1706.2 ± 630.6***	256.9 ± 66.46***
SH-SY5Y	TCP	505.2 ± 150.4	158.6 ± 40.2
	Coll	842.8 ± 343.1	179.5 ± 49.3
IMR-32	TCP	554.3 ± 206.5	142 ± 27.9
	Coll	878.7 ± 444.7	182.6 ± 46.4

* $p<0.05$

*** $p<0.001$